International Journal of Thermophysics

Supplementary Material

Thermophysical Properties of Alkali Metals: A Partition Function Theory Approach Including Low-Lying Electronic States

Carlos D. da Silva[a], Marcos D. S,
Ramon S. da Silva[a], Maikel Y. Ballester

Departamento de Física, Instituto de Ciências Exatas – ICE,
Universidade Federal de Juiz de Fora,
Rua José Lourenço Kelmer, s/n, Juiz de Fora,
36036-330, Minas Gerais, Brasil

maikel.ballester@ufjf.br

1 Analytical Form of the Interatomic Potentials

The analytical form employed in the fitting procedure is based on the Extended Hartree-Fock Approximate Correlation Energy (EHFACE) Method, proposed by da Silva and Varandas [1]. In essence, the potential energy is decomposed into a short-range term and a long-range term:

$$U(R) = u_{EHF}(R) + u_{dc}(R) \tag{1}$$

The short-range term or Extended Hartree-Fock (EHF) term is written as

$$u_{EHF}(r) = -\frac{D}{R}\left(1 + \sum_{i=1}^{n} a_i r^i\right)\exp(-r\gamma(r)) \tag{2}$$

$$\gamma(r) = \gamma_0[1 + \gamma_1 \tanh(\gamma_2 r)] \tag{3}$$

where $r = R - R_e$. The parameters D, a_i, e γ_i are ajustable. The long-range part of EHFACE potential or dynamic correlation (dc) term is given by

$$u_{dc}(R) = -\sum_{n=6,8,10}^{N} \chi_n(R)\frac{C_n}{R^n} \tag{4}$$

where C_n represent the dispersion coefficients and $\chi_n(R)$ is the damping function given by

$$\chi_n(R) = \left[1 - \exp\left(-\frac{A_n R}{\rho} - \frac{B_n R^2}{\rho^2}\right)\right]^n \tag{5}$$

Furthermore, A_n and B_n are auxiliary functions and are written as $A_n = \alpha_0 n^{-\alpha_1}$ and $B_n = \beta_0 \exp(-\beta_1)$, with $\alpha_0, \alpha_1, \beta_0$ and β_1 being universal dimensional parameters for all isotropic interactions: α_0 = 16.36606, α_1 = 0.70172, β_0 = 17.19338, and β_1 = 0.09574. In turn, for the MN atomic pair, $\rho/\alpha_0 = 5.5 + 1.25\mathrm{R}_0$, where $R_0 = 2(< r_M^2 >^{\frac{1}{2}} + < r_N^2 >^{\frac{1}{2}})$ is the LeRoy parameter. $< r_M^2 >$ and $< r_N^2 >$ are the expected values of the square radii for the outermost electron in the M and N atoms, respectively. The EHFACE model guarantees the correct asymptotic limits $R \to \infty$ and $R \to 0$.

2 Low Lying Electronic States

2.1 Model Formulation

In this work, we consider a system of N indistinguishable, non-interacting diatomic molecules confined in a volume V and in thermal equilibrium at temperature T. The microscopic description of the system is developed within both classical and quantum statistical mechanics, starting from the construction of the total Hamiltonian and the corresponding partition function. Each molecule is assumed to be independent, with its total Hamiltonian separable into translational and internal contributions. We adopt a canonical coordinate system (q, p), where the translational degrees of freedom are described by the center-of-mass coordinate $\vec{R}_{\mathrm{cm}} \in \mathbb{R}^3$ and its conjugate momentum $\vec{P}_{\mathrm{cm}}$, while the internal degrees of freedom are given by $q' = (r, \theta, \phi)$, representing the internuclear distance and spherical angles defining the molecular orientation, with conjugate momenta $p' = (p_r, p_\theta, p_\phi)$. The total Hamiltonian operator in quantum description can be expressed as:

$$\begin{aligned}\hat{\mathcal{H}} &= \hat{T}_{\text{tr}} + \hat{\mathcal{H}}_{\text{int}} \\ &= -\frac{\hbar^2}{2m}\nabla^2_{\text{cm}} + -\frac{\hbar^2}{2\mu}\frac{d^2}{dr^2} + U_n(r) + \frac{\hbar^2}{2\mu r^2}\left[J(J+1) - \Lambda^2\right]\end{aligned} \tag{6}$$

where m is the total mass of the molecule, μ is the reduced mass, $U_n(r)$ is the electronic potential energy curve for the electronic state n, J is the total angular momentum quantum number, and Λ is the absolute value of the electronic angular momentum projection onto the internuclear axis. Non-adiabatic couplings and spin-orbit interactions are neglected. The corresponding classical Hamiltonian reads:

$$\begin{aligned}\mathscr{H} &= \mathscr{T}_{\text{tr}} + \mathscr{H}_{\text{int}} \\ &= \frac{1}{2m}P^2_{\text{cm}} + \left[\frac{p_r^2}{2\mu} + U_n(r) + \frac{1}{2\mu r^2}\left(p_\theta^2 + \frac{p_\phi^2}{\sin^2\theta}\right)\right]\end{aligned} \tag{7}$$

where the rotational kinetic energy is implicitly expressed through the moment of inertia $I = \mu r^2$. With the Hamiltonians defined, the quantum canonical partition function is written as:

$$Q^{\text{qm}}(T,V,N) = \frac{1}{N!}\left[\frac{V}{\lambda_T^3}\sum_n g_n \sum_{v,J} g_J^n \exp\left(-\frac{\mathcal{E}_{n,v,J}}{k_B T}\right)\right]^N \tag{8}$$

where $\lambda_T = h/\sqrt{2\pi m k_B T}$ is the thermal wavelength, $\mathcal{E}_{n,v,J}$ represents the total molecular energy in the electronic (n), vibrational (v), and rotational (J) levels, g_n is the degeneracy of the electronic state, and g_J^n is the rotational degeneracy factor. Alternatively, the classical partition function is given by:

$$\begin{aligned}Q_{\text{cl}}(T,V,N) &= \frac{1}{N!}\left[\frac{1}{h^3}\int_{\mathbb{R}^3} d^3R_{\text{cm}} \int_{\mathbb{R}^3} d^3P_{\text{cm}} \exp\left(-\frac{P^2_{\text{cm}}}{2mk_BT}\right)\times\right. \\ &\qquad \left.\times \sum_n g_n \int_{\Omega_{q'}} dq' \int_{\Omega_{p'}} dp' \exp\left(-\frac{\mathscr{H}^n_{\text{int}}(p',q')}{k_BT}\right)\right]^N \\ &= \frac{1}{N!}\left[\frac{V}{\lambda_T^3}\sum_n g_n \int_{\Omega_{q'}} dq' \int_{\Omega_{p'}} dp' \exp\left(-\frac{\mathscr{H}^n_{\text{int}}(p',q')}{k_BT}\right)\right]^N \\ &= \frac{1}{N!}\left[\frac{V}{\lambda_T^3}\sum_n \frac{g_n}{2\sqrt{\pi}}(2\mu k_BT)^{3/2}\int_0^\infty \left[\exp\left(-\frac{U_n(r)}{k_BT}\right) - 1\right] r^2\,\mathrm{d}r\right]^N\end{aligned} \tag{9}$$

This classical formulation becomes valid when the energy levels are densely spaced, allowing for a continuous approximation (typically when $k_BT \gg \Delta\mathcal{E}$, with $\Delta\mathcal{E}$ the level spacing), the final result is expressed in reduced units [2, 3]. The integration domains cover the full phase space of internal degrees of freedom, with $\Omega_{q'} = [0,\infty) \times [0,\pi] \times [0,2\pi)$ and $\Omega_{p'} = \mathbb{R}^3$.

2.2 Assumptions and Limitations

For each dissociative channel considered for alkali metal dimers, the equilibrium can be formally represented by the reversible process:

$$A_2(\alpha) \rightleftharpoons A(\alpha') + A(\alpha'') \tag{10}$$

where α, α', and α'' denote the relevant internal states of the molecular and atomic species involved [4]. In this framework, the total internal partition function $Q_{\rm int}$ can be decomposed into the sum of three distinct contributions: the bound-state contribution $Q^B_{\rm int}$, the contribution from continuum $Q^C_{\rm int}$ is separed in metastable or quasi-bound states $Q^M_{\rm int}$, and the free contribution $Q^F_{\rm int}$ [4, 5], such that

$$\begin{aligned} Q_{\rm int}(T) &= Q^B_{\rm int}(T) + Q^C_{\rm int}(T) \\ &= Q^B_{\rm int}(T) + Q^M_{\rm int}(T) + Q^F_{\rm int}(T) \end{aligned} \tag{11}$$

The classical expression for the internal partition function, obtained by integrating over the entire phase space, naturally includes all three contributions within $Q^{\rm cl}_{\rm int}$. For electronic bound-state potentials $U_n(r)$, there exists a finite distance σ such that $U_n(\sigma) = 0$. In the region $r \in [0, \sigma)$, the potential energy is positive, $U_n(r) > 0$, and thus the $Q^{\rm cl}_{\rm int} < 0$. Conversely, in the region $r \in [\sigma, \infty)$, where $U_n(r) \leq 0$, the contribution is $Q^{\rm cl}_{\rm int} > 0$. Therefore, the classical partition function contains both negative and positive contributions depending on the integration domain. This approach captures the three possible contributions of bound, metastable, and free states to the internal partition function of alkali metal dimers [4]. However, at low temperatures, the classical description fails to quantitatively reproduce the physical behavior of the system, as it neglects the quantum nature of the molecular energy levels. In this regime, the thermal energy becomes comparable to or smaller than the spacing between energy eigenvalues, making the continuous approximation of energy, inherent to the classical partition function, invalid. Therefore, a quantum mechanical description of the system becomes necessary, requiring the use of the quantum partition function to accurately account for the discrete energy levels.

The quantum expression for the internal partition function, $Q^{\rm qm}_{\rm int}$, typically includes only the contribution from bound states, neglecting the metastable and free state contributions. This approximation is justified by the fact that, for electronic states with sufficiently deep potential wells $Q^B_{\rm int}(T) \gg Q^M_{\rm int}(T)$. The number of metastable states, which may exist behind centrifugal barriers, is generally small and becomes negligible for deeply bound electronic states. Moreover, $Q^B_{\rm int}(T) > Q^F_{\rm int}(T)$. Therefore, in this work, the quantum description of the internal partition function is restricted to the sum over bound states. This assumption remains valid for the range of temperatures considered here, as the total contribution from bound levels is expected to be significantly larger than the combined contributions from metastable and continuum states for the electronic states investigated. The limitations of the model adopted in this work arise from fundamental approximations made to ensure computational feasibility and internal consistency of the physical assumptions. First, the system is assumed to be in thermal equilibrium, which allows the use of well defined statistical distributions to describe the population of energy states. Additionally, the ideal gas approximation is adopted, meaning that intermolecular interactions are neglected. Finally, not all electronic states of each dissociative channel were included. In particular, purely repulsive states and those associated with complex potential energy curves, such as double-well potentials, were excluded. Including such states which are often poorly characterized or lack reliable spectroscopic data could introduce significant uncertainties into the internal partition function. Since this function directly influences the resulting thermodynamic and population properties, its construction was deliberately limited to well defined bound states, in order to preserve the physical reliability and consistency of the model within the acceptable limits of precision.

2.3 Relative Error Associated with Rovibrational Energy Splitting in the Partition Function at High Temperatures

In this section, we examine the relative error introduced in the internal partition function when using simplified rovibrational energy splittings, particularly in systems with low-lying electronic states, at high temperatures. The internal partition function, computed via quantum mechanical methods, includes contributions from electronic, vibrational, and rotational energy levels. However, at elevated temperatures, neglecting or inaccurately treating the contribution of electronically excited states can lead to deviations. We evaluate the magnitude of this error and its dependence on the energetic proximity of these states, aiming to quantify how such simplifications impact the accuracy of thermodynamic predictions.

Consider the internal partition function obtained by the quantum mechanical methods:

$$Q_{\text{int}}(T) = \sum_{n=1}^{n_{\max}} g_n \sum_{v=0}^{v_{\max}(n)} \left[\sum_{J \in 2\mathbb{N}_0}^{J_{\text{even,max}}(n)} g_{nuc}^{\text{even}} (2J+1) \exp\left(-\frac{\mathcal{E}_{n,v,J}}{k_B T}\right) + \sum_{J \in 2\mathbb{N}_0+1}^{J_{\text{odd,max}}(n)} g_{nuc}^{\text{odd}} (2J+1) \exp\left(-\frac{\mathcal{E}_{n,v,J}}{k_B T}\right) \right] \tag{12}$$

We can rewrite it in a simplified form using: $\mathcal{E}_{n,v,J} = \mathcal{E}_n^{el} + \mathcal{E}_{n,v}^{vib} + \mathcal{E}_{n,v,J}^{rot}$

$$\begin{aligned} Q_{\text{int}}(T) &:= \sum_n g_n \sum_{v,J} g_J^n \exp\left(-\frac{\mathcal{E}_{n,v,J}}{k_B T}\right) \\ &= \sum_n g_n \exp\left(-\frac{\mathcal{E}_n^{\text{el}}}{k_B T}\right) \sum_{v,J} g_J^n \exp\left(-\frac{\mathcal{E}_{n,v}^{\text{vib}} + \mathcal{E}_{n,v,J}^{\text{rot}}}{k_B T}\right) \end{aligned} \tag{13}$$

Let $\mathcal{E'}_{n,v,J} = \mathcal{E}_{n,v,J} + \delta_{n,v,J}$, where $\mathcal{E}_{n,v,J}$ is the true energy and $\delta_{n,v,J}$ is the splitting. We then have an approximate partition function given by

$$\begin{aligned} Q'_{\text{int}}(T) &= \sum_n g_n \sum_{v,J} g_J^n \exp\left(-\frac{\mathcal{E'}_{n,v,J}}{k_B T}\right) \\ &= \sum_n g_n \exp\left(-\frac{\mathcal{E}_n^{\text{el}}}{k_B T}\right) \sum_{v,J} g_J^n \exp\left(-\frac{\mathcal{E}_{n,v}^{\text{vib}} + \mathcal{E}_{n,v,J}^{\text{rot}} + \delta_{n,v,J}}{k_B T}\right) \\ &= \sum_n g_n \exp\left(-\frac{\mathcal{E}_n^{\text{el}}}{k_B T}\right) \sum_{v,J} g_J^n \exp\left(-\frac{\mathcal{E}_{n,v}^{\text{vib}} + \mathcal{E}_{n,v,J}^{\text{rot}}}{k_B T}\right) \exp\left(-\frac{\delta_{n,v,J}}{k_B T}\right) \end{aligned} \tag{14}$$

Assuming that $|\delta_{n,v,J}| \ll k_B T$ and applying the first-order Taylor expansion of the exponential, we have:

$$\exp\left(-\frac{\delta_{n,v,J}}{k_B T}\right) = 1 - \frac{\delta_{n,v,J}}{k_B T} + O((\delta_{n,v,J}/k_B T)^2) \tag{15}$$

neglecting higher-order terms, we obtain a first-order approximation for the corrected partition function:

$$Q'_{\rm int}(T) \approx \sum_n g_n \exp\left(-\frac{\mathcal{E}_n^{\rm el}}{k_B T}\right) \sum_{v,J} g_J^n \exp\left(-\frac{\mathcal{E}_{n,v}^{\rm vib} + \mathcal{E}_{n,v,J}^{\rm rot}}{k_B T}\right)\left(1 - \frac{\delta_{n,v,J}}{k_B T}\right)$$
$$= Q_{\rm int}(T) - \frac{1}{k_B T} \sum_{n,v,J} \delta_{n,v,J}\, g_n\, g_J^n\, \exp\left(-\frac{\mathcal{E}_{n,v,J}}{k_B T}\right) \tag{16}$$

defining relative error as:

$$\varepsilon_{\rm rel} := \left| \frac{Q_{\rm int} - Q'_{\rm int}}{Q_{\rm int}} \right| \tag{17}$$

Thus, the first order approximation for the relative error is given by:

$$\varepsilon_{\rm rel} \approx \frac{1}{k_B T} \frac{1}{Q_{\rm int}} \sum_{n,v,J} \delta_{n,v,J} g_n g_J^n \exp\left(-\frac{\mathcal{E}_{n,v,J}}{k_B T}\right) \tag{18}$$

that is

$$\varepsilon_{\rm rel} \approx \frac{1}{k_B T} < \delta_{n,v,J} > \tag{19}$$

this last expression is important because it shows that the relative error caused by a relatively large splitting leads to a small error at high temperatures, a regime where the low-lying electronic states are significantly populated. In this work, the electronic states of the first dissociative channel must be described with accurate potential energy curves, as they can induce significant relative errors at low temperatures. Although our focus is on high-temperature regimes, the cumulative relative errors arising from the electronic states of the other dissociative channels may still be non-negligible. Therefore, even though the relative error tends to decrease at elevated temperatures, a precise representation of the system's energy eigenvalues remains essential. This is not only to minimize errors but also to ensure an accurate counting of the bound states within the system.

2.4 Thermal Population of Low-Lying States at High Temperatures

The population of the electronic state n is given by:

$$P_n(T) \propto g_n \exp\left(-\frac{\mathcal{E}_{n,v,J}}{k_B T}\right) \sum_{v,J} g_J^n \exp\left(-\frac{\mathcal{E}_{n,v}^{\rm vib} + \mathcal{E}_{n,v,J}^{\rm rot}}{k_B T}\right) \tag{20}$$

at high temperatures, where the rovibrational energy is small compared to the thermal energy $\mathcal{E}_{v,J} = \mathcal{E}_{n,v}^{\rm vib} + \mathcal{E}_{n,v,J}^{\rm rot} \ll k_B T$ can expand the exponential in a Taylor series, we have:

$$\exp\left(-\frac{\mathcal{E}_{v,J}}{k_B T}\right) = 1 - \frac{\mathcal{E}_{v,J}}{k_B T} + O((\mathcal{E}_{v,J}/k_B T)^2) \tag{21}$$

neglecting higher-order terms, we obtain a first-order approximation:

$$P_n(T) \propto g_n \exp\left(-\frac{\mathcal{E}_{n,v,J}}{k_B T}\right) \sum_{v,J} g_J^n \left(1 - \frac{\mathcal{E}_{v,J}}{k_B T}\right) \tag{22}$$

where the electronic degeneracy is given by:

$$g_n = (2 - \delta_{\Lambda_n,0})(2S_n + 1), \tag{23}$$

accounting for spin multiplicity and the projection Λ_n of the electronic angular momentum along the internuclear axis. In this regime, the dominant factor controlling the population $P_n(T)$ of an electronic state n is the electronic excitation energy $\mathcal{E}_n^{\text{elec}}$,electronic degeneracy $g_n = (2 - \delta_{\Lambda_n,0})(2S_n + 1)$ and the total number of vibrational and rotational states.

Another rigorous conclusion at high temperature concerns the number of bound rovibrational states that contribute to the partition function. For a given electronic state n, the total number of vibrational and rotational levels is finite and determined by the depth of the electronic potential well $D_e^{(n)}$. At high temperatures, more states become thermally accessible, and the number of contributing rovibrational states increases. The total contribution to the internal partition function of state n can be approximated as: which must both be small. This justifies the truncation of the exponential and explains why the electronic structure becomes the principal determinant of thermodynamic populations at sufficiently high T. Hence, at high T, the magnitude of this sum depends on the depth of the potential energy curve $D_e^{(n)}$ and the density of states within this well, consequently depends on the value of spectroscopic parameters which altogether can determine how many states satisfy $\mathcal{E}_{n,v,J} < D_e^{(n)}$ and are thus physically bound. These factors collectively determine how many bound rovibrational states are thermally populated at a given temperature. Importantly, even when two electronic states have similar electronic excitation energies $\mathcal{E}_n^{\text{elec}}$, the state with the deeper potential well will typically contribute more significantly to the total partition function at high temperatures, due to the larger number of accessible bound states. This highlights a key insight: the effective statistical weight of an electronic state at elevated temperatures is not solely defined by its electronic degeneracy and excitation energy, but also by the number of rovibrational states it supports a structural characteristic encoded in the shape and depth of its potential energy curve.

2.5 Nuclear Spin Degeneracy in Partition Functions

The calculation of molecular partition functions requires careful consideration of nuclear spin degeneracy, which arises due to the quantum mechanical properties of identical nuclei within a molecule. Specifically, for molecules composed of identical atoms, the symmetry of the total nuclear spin wavefunction influences the number of accessible quantum states, depending on whether the combined nuclear spin states are symmetric (even) or antisymmetric (odd) under particle exchange. This distinction affects the statistical weight of each molecular state and is captured by the nuclear spin degeneracy factors $g_{nuc}^{odd/even}$, defined as

$$g_{nuc,n}^{odd/even} = \frac{1}{2}\left[(2I+1)^2 \pm (2I+1)\right] \tag{24}$$

or in terms of the weight of rotational nuclear degeneracy:

$$g_{nuc,n}^{\text{even / odd}} = \frac{(2I+1)^2 \pm (2I+1)}{2(2I+1)^2} \tag{25}$$

The odd/even degeneracy ratio is normalized in the statistical symmetry table, typically represented as Tab.S1, which specifies how the degeneracies should be handled, taking into account nuclear spin effects and the system symmetry. The normalization ensures that the contributions from different degeneracies are properly adjusted to accurately and consistently calculate the possible states.

1

[1]Table S1 has been adapted from Ref. [6], preserving the correlation between statistical symmetry, electronic configuration, and the parity.

Table S1: Nuclear degeneracy in homonuclear molecules arises from the correlation between statistical symmetry, electronic configuration, and the parity of J. The signs indicate whether addition or subtraction rules apply.

Statistical Symmetry	**Electronic Configuration**	**Parity sign of J**
Fermi-Dirac (**Antisymmetric**) Nuclear Spin: I Half-Integral	Σ_g^+, Σ_u^-	Odd $+$
		Even $-$
	Σ_u^+, Σ_g^-	Odd $-$
		Even $+$
	Non-Sigma State: Nuclear weights are equal for both parity of J	
Bose-Einstein (**Symmetric**) Nuclear Spin: I Integral	Σ_g^+, Σ_u^-	Odd $-$
		Even $+$
	Σ_u^+, Σ_g^-	Odd $+$
		Even $-$
	Non-Sigma State: Nuclear weights are equal for both parity of J	

2.6 When Statistical Descriptions of Diatomic Systems Reach Convergence

For Fermi–Dirac or Bose–Einstein statistics including nuclear spin degeneracy, the internal partition function of an diatomic molecule at sufficiently high temperatures can be approximated as

$$Q_{\text{int}}^{F/B}(T) = \sum_n g_n \exp\left(-\frac{\mathcal{E}_n^{\text{el}}}{k_B T}\right) \sum_{v=0}^{v_{\max}(n)} \exp\left(-\frac{\mathcal{E}_{n,v}^{\text{vib}}}{k_B T}\right) \times \left[\sum_{J\in 2\mathbb{N}_0}^{J_{\text{even,max}}(n)} g_{\text{nuc}}^{\text{even}}(2J+1)\exp\left(-\frac{\mathcal{E}_{n,v,J}^{\text{rot}}}{k_B T}\right) + \sum_{J\in 2\mathbb{N}_0+1}^{J_{\text{odd,max}}(n)} g_{\text{nuc}}^{\text{odd}}(2J+1)\exp\left(-\frac{\mathcal{E}_{n,v,J}^{\text{rot}}}{k_B T}\right)\right]. \tag{26}$$

The rotational part of the internal partition function can thus be written as:

$$Q_{\text{rot}}^{F/B}(T) = \sum_{J\in 2\mathbb{N}_0}^{J_{\text{even,max}}(n)} g_{\text{nuc}}^{\text{even}}(2J+1)\exp\left(-\frac{\mathcal{E}_{n,v,J}^{\text{rot}}}{k_B T}\right) + \sum_{J\in 2\mathbb{N}_0+1}^{J_{\text{odd,max}}(n)} g_{\text{nuc}}^{\text{odd}}(2J+1)\exp\left(-\frac{\mathcal{E}_{n,v,J}^{\text{rot}}}{k_B T}\right). \tag{27}$$

At high temperatures, where the condition $\mathcal{E}_{n,v,J}^{\text{rot}} \ll k_B T$ holds, the rotational partition function simplifies to

$$
\begin{aligned}
Q_{\mathrm{rot}}^{F/B}(T) &\xrightarrow{T\to\infty} \sum_{J\in 2\mathbb{N}_0}^{J_{\mathrm{even,max}}(n)} g_{\mathrm{nuc}}^{\mathrm{even}}(2J+1) + \sum_{J\in 2\mathbb{N}_0+1}^{J_{\mathrm{odd,max}}(n)} g_{\mathrm{nuc}}^{\mathrm{odd}}(2J+1) \\
&\approx g_{\mathrm{nuc}}^{\mathrm{even}} \sum_{J\in 2\mathbb{N}_0}^{J_{\mathrm{even,max}}(n)} (2J+1) + g_{\mathrm{nuc}}^{\mathrm{odd}} \sum_{J\in 2\mathbb{N}_0+1}^{J_{\mathrm{odd,max}}(n)} (2J+1) \\
&\approx \frac{1}{2}\left(g_{\mathrm{nuc}}^{\mathrm{even}} + g_{\mathrm{nuc}}^{\mathrm{odd}}\right) \sum_{J=0}^{J_{\mathrm{max}}(n)} (2J+1) \\
&\approx \frac{1}{2}(2I+1)^2 \sum_{J=0}^{J_{\mathrm{max}}(n)} (2J+1) \\
&\approx \frac{1}{2} Q_{\mathrm{rot}}^{MB}(T), \qquad (28)
\end{aligned}
$$

where, for homonuclear diatomic molecules, the total nuclear spin degeneracy is given by $g_{\mathrm{nuc}} = (2I+1)^2$. This result demonstrates that, in the high-temperature limit, the rotational partition function under Fermi–Dirac or Bose–Einstein statistics for homonuclear molecules becomes equal to half of the classical Maxwell–Boltzmann rotational partition function. This reduction symmetric factor 1/2, is not an arbitrary adjustment in the Maxwell–Boltzmann description. Instead, it naturally emerges from the indistinguishability of particles and the quantum symmetrization requirements of nuclear spin states under Fermi–Dirac and Bose–Einstein statistics. This symmetrization effectively reduces the number of accessible rotational states by half compared to the classical Maxwell–Boltzmann statistics, which do not consider such quantum effects and thus omit the 1/2 factor in state counting. Furthermore, at high temperatures, the Fermi–Dirac and Bose–Einstein statistics converge to the Maxwell–Boltzmann distribution, validating the classical approximation in this limit while preserving the impact of the symmetrization factor on the effective state degeneracy.

2.7 Analysis of Ground Electronic State Thermodynamic Properties for Alkali Dimers

In this subsection, a quantitative evaluation of the thermodynamic properties of alkali metal dimers in their electronic ground states is presented, based on the computational methods developed in this work. The properties considered include the Gibbs free energy, enthalpy, entropy, and constant pressure heat capacity, all computed over the temperature range of 300–2000 K using a uniform grid of 170 points. The results obtained from each method are compared against experimental reference data from the JANAF Thermochemical Tables, as compiled by Chase (1998) and made available through the NIST database. The selected temperature range ensures the analysis remains confined to the regime in which only the first dissociation channel is relevant and the ground electronic state predominates. Table S2 presents the absolute and relative root-mean-square errors (RMSE ABS and RMSE%) associated with each thermodynamic property and computational method, providing a clear metric for assessing model accuracy. The RMSE ABS is defined as the square root of the mean squared deviation between the predicted and reference values, while RMSE% is calculated by normalizing RMSE ABS with respect to the mean reference value and expressing the result as a percentage.

$$\text{RMSE ABS} = \sqrt{\frac{1}{n}\sum_{i=1}^{n}(y_i - \bar{y}_i)^2} \quad \text{and} \quad \text{RMSE \%} = \left(\frac{\text{RMSE}}{\bar{y}}\right) \times 100 \tag{29}$$

In these equations, y_i represents the value predicted by the model at the i-th temperature point, $\bar{y}_i$ denotes the corresponding reference value (e.g., experimental or tabulated), n is the total number of points considered, $\bar{y}$ is the arithmetic mean of the reference values over the entire temperature range. These definitions provide a quantitative measure of the deviation between the computed and reference thermodynamic properties, both in absolute terms and as a percentage relative to the magnitude of the reference data.

Table S2: Absolute (RMSE ABS.) and relative (RMSE %) root mean square error for the thermodynamic properties of alkali metals calculated using the methods developed in this work.

Alkali Metal	**Method**	Cp **(ABS / %)**	$H - H^{\circ}_{298\,K}$ **(ABS / %)**	S **(ABS / %)**	$-(G - H_{298K})/T$ **(ABS / %)**
Li_2	1	1.04 / 2.77	0.57 / 1.78	0.42 / 0.17	0.09 / 0.04
	2	0.96 / 2.56	0.26 / 0.80	6.60 / 2.71	6.43 / 2.94
	3	3.11 / 8.27	2.21 / 6.84	–	–
	4	3.28 / 8.72	1.57 / 4.85	–	–
Na_2	1	0.57 / 1.52	0.53 / 1.62	0.74 / 0.27	1.03 / 0.41
	2	0.52 / 1.39	0.39 / 1.20	8.18 / 2.95	7.86 / 3.12
	3	2.31 / 6.19	0.93 / 2.85	–	–
	4	2.43 / 6.50	1.02 / 3.13	–	–
K_2	1	0.26 / 0.76	0.07 / 0.24	1.06 / 0.36	1.06 / 0.39
	2	0.38 / 1.11	0.11 / 0.36	4.56 / 1.54	4.61 / 1.70
	3	3.23 / 9.56	1.21 / 3.93	–	–
	4	3.24 / 9.61	1.20 / 3.91	–	–
Rb_2	1	0.88 / 2.72	0.81 / 2.71	2.02 / 0.64	1.48 / 0.51
	2	0.55 / 1.69	0.07 / 0.22	5.43 / 1.72	5.37 / 1.84
	3	1.70 / 5.25	1.54 / 5.16	–	–
	4	1.71 / 5.28	1.54 / 5.17	–	–
Cs_2	1	0.49 / 1.54	0.17 / 0.58	4.68 / 1.42	4.82 / 1.57
	2	0.53 / 1.65	0.36 / 1.20	5.91 / 1.79	5.74 / 1.88
	3	1.36 / 4.27	0.97 / 3.27	–	–
	4	1.37 / 4.29	0.97 / 3.28	–	–
Mean (170 points, 300–2000 K)				Compared with Chase 1998 [7]	

A comparative analysis between methods 1 and 2 revealed a root mean square percentage error (RMSE%) lower than 3.12% within the considered temperature range. This result demonstrates that, given the adopted spectroscopic parameters, the Dunham expansion constitutes a reliable strategy for calculating energy eigenvalues and associated thermodynamic properties. Nevertheless, it was identified that the applicability of this approach becomes intrinsically constrained at elevated temperatures, where the partial population of higher energy states becomes significant. Under these conditions, the truncation of the Dunham expansion—particularly the omission of higher-order rovibrational coupling terms—compromises the accurate representation of the molecular energy structure, leading to systematic deviations. Conversely, the classical approach (method 3) and the semiclassical formulation incorporating second-order Wigner-Kirkwood corrections (method 4) exhibited considerably higher RMSE% values at low

temperatures. This discrepancy primarily arises from the inability of these methods to account for the quantization of energy levels, which is especially relevant in the ground-state regime. As a consequence, these approximations prove inadequate for an accurate description of thermodynamic properties at low temperatures. Despite the formal validity of the semiclassical corrections, their inclusion did not result in significant improvements in the computed thermodynamic quantities, indicating a negligible practical impact in temperature regimes where quantum effects predominate.

2.8 Translational and Internal Contributions of Low Lying States

The ability to separate thermal properties into translational and internal components through the partition function formalism is fundamental for a detailed understanding of molecular behavior. This decomposition allows us to evaluate the relative contributions of different degrees of freedom, electronic states to the overall thermodynamic properties. By comparing these contributions across temperature ranges, we can assess the regimes where internal degrees of freedom become significant and when the system approaches ideal gas behavior. Notably, the imperfect gas model serves as a viable approximation in temperature intervals where internal contributions are substantial but still compatible with the assumptions of weak intermolecular interactions. Such an approach is essential for accurately modeling the thermodynamics of alkali metal dimers and predicting their behavior under various conditions. The results for these translational and internal contributions to the thermodynamic functions are presented below. Assuming that the total partition function can be factorized into translational and internal contributions:

$$Q(T) = Q_{\text{trans}}(T) \cdot Q_{\text{int}}(T), \tag{30}$$

The molar entropy $S(T)$ can be expressed as:

$$\begin{aligned} S(T) &= R \ln Q(T) + RT \frac{d \ln Q(T)}{dT} \\ &= \underbrace{R \ln Q_{\text{trans}} + RT \frac{d \ln Q_{\text{trans}}}{dT}}_{S_{\text{trans}}(T)} + \underbrace{R \ln Q_{\text{int}} + RT \frac{d \ln Q_{\text{int}}}{dT}}_{S_{\text{int}}(T)} \\ &= S_{\text{trans}}(T) + S_{\text{int}}(T) \end{aligned} \tag{31}$$

The enthalpy $H(T)$ is obtained as:

$$\begin{aligned} H(T) &= RT^2 \frac{d \ln Q(T)}{dT} \\ &= \underbrace{RT^2 \frac{d \ln Q_{\text{trans}}}{dT}}_{H_{\text{trans}}(T)} + \underbrace{RT^2 \frac{d \ln Q_{\text{int}}}{dT}}_{H_{\text{int}}(T)} \\ &= H_{\text{trans}}(T) + H_{\text{int}}(T) \end{aligned} \tag{32}$$

The Gibbs free energy $G(T)$ is:

$$
\begin{aligned}
G(T) &= H(T) - TS(T) \\
&= \underbrace{H_{\text{trans}}(T) - TS_{\text{trans}}(T)}_{G_{\text{trans}}(T)} + \underbrace{H_{\text{int}}(T) - TS_{\text{int}}(T)}_{G_{\text{int}}(T)} \\
&= G_{\text{trans}}(T) + G_{\text{int}}(T)
\end{aligned} \tag{33}
$$

Finally, the heat capacity at constant pressure $C_p(T)$ is given by:

$$
\begin{aligned}
C_p(T) &= \underbrace{RT\frac{d^2}{dT^2}\left[T \ln Q_{\text{int}}(T)\right]}_{C_{p,\text{int}}(T)} + \underbrace{\frac{5}{2}R}_{C_{p,\text{trans}}} \\
&= C_{p,\text{trans}}(T) + C_{p,\text{int}}(T)
\end{aligned} \tag{34}
$$

These expressions allow a clear separation of translational and internal contributions to the thermodynamic functions, which is particularly useful in molecular simulations or when evaluating vibrational, rotational, and electronic effects independently. To quantify the relative contribution of each component, the internal contribution can be expressed as a percentage of the total value as:

$$
\begin{aligned}
\text{Entropy:} \quad & \frac{S_{\text{trans}}(T)}{S(T)} \times 100 = S_{\text{trans}}^{(\%)}, \quad \frac{S_{\text{int}}(T)}{S(T)} \times 100 = S_{\text{int}}^{(\%)} \\
\text{Enthalpy:} \quad & \frac{H_{\text{trans}}(T)}{H(T)} \times 100 = H_{\text{trans}}^{(\%)}, \quad \frac{H_{\text{int}}(T)}{H(T)} \times 100 = H_{\text{int}}^{(\%)} \\
\text{Gibbs free energy:} \quad & \frac{G_{\text{trans}}(T)}{G(T)} \times 100 = G_{\text{trans}}^{(\%)}, \quad \frac{G_{\text{int}}(T)}{G(T)} \times 100 = G_{\text{int}}^{(\%)} \\
\text{Heat capacity:} \quad & \frac{C_{p,\text{trans}}}{C_p(T)} \times 100 = C_{p,\text{trans}}^{(\%)}, \quad \frac{C_{p,\text{int}}(T)}{C_p(T)} \times 100 = C_{p,\text{int}}^{(\%)}
\end{aligned} \tag{35}
$$

For the lithium dimer, the analysis of C_p rewriting the thermal properties in translational and internal terms reveals a consistent predominance of the internal contribution $C_{p,\text{int}}$ over the translational component $C_{p,\text{tr}}$ throughout the investigated temperature range. This distinction becomes particularly pronounced at elevated temperatures, especially above 2000 K. In the lower temperature regime, between 300 K and 2000 K, the internal degrees of freedom already contribute significantly to the total heat capacity. Specifically, the fractional contribution of $C_{p,\text{int}}$ to the total C_p ranges from a minimum of 53.14% to a maximum of 57.78% within this interval. These values indicate that even at moderate temperatures, the internal structure of the Li_2 molecule plays a non-negligible role in its thermal behavior, exceeding the contribution from pure translational motion. Above 2000 K, this trend intensifies markedly. The elevated thermal energy at such temperatures increasingly populates internal energy levels, enhancing the internal energy fluctuations and, consequently, the heat capacity associated with internal degrees of freedom. In this high temperature regime T > 2000K, the condition $C_{p,\text{int}} > C_{p,\text{tr}}$ holds consistently. Quantitatively, within the temperature range of 4000 K to 6000 K, the internal contribution accounts for approximately 70.69% to 72.42% of the total heat capacity. With respect to enthalpy, the translational contribution H_{tr} is the dominant term throughout most of the temperature range investigated. At 300 K, it reaches its maximum relative contribution, accounting for approximately 65.20% of the total enthalpy. As temperature increases,

this percentage gradually decreases, although H_{tr} remains the largest single contributor up to a temperature of 4040 K. At precisely 4040 K, a notable transition occurs: the translational and internal contributions H_{tr} and H_{int} become equal in magnitude. Beyond this temperature, the internal enthalpy component H_{int} surpasses the translational one. This crossover marks a significant shift in the energy distribution within the system, indicating the increasing importance of internal energy level excitations at elevated temperatures. Importantly, this transition helps to explain the deviation observed between theoretical and experimental enthalpy values for lithium dimer at high temperatures when calculations consider only the ground electronic state. The neglect of thermally accessible excited states can lead to underestimation of H_{int}, particularly above 4040 K, where its contribution becomes dominant. For entropy and Gibbs free energy, similar analyses were carried out across the alkali metal dimers (see figure S1 in SM for more details). In all cases examined, translational contributions to entropy S_{tr} and Gibbs energy G_{tr} remain dominant throughout the studied temperature range. However, the internal terms S_{int} and G_{int} exhibit a clear and progressive increase with temperature, reflecting the gradual population of higher internal states and their growing influence on the thermodynamic behavior of the systems.

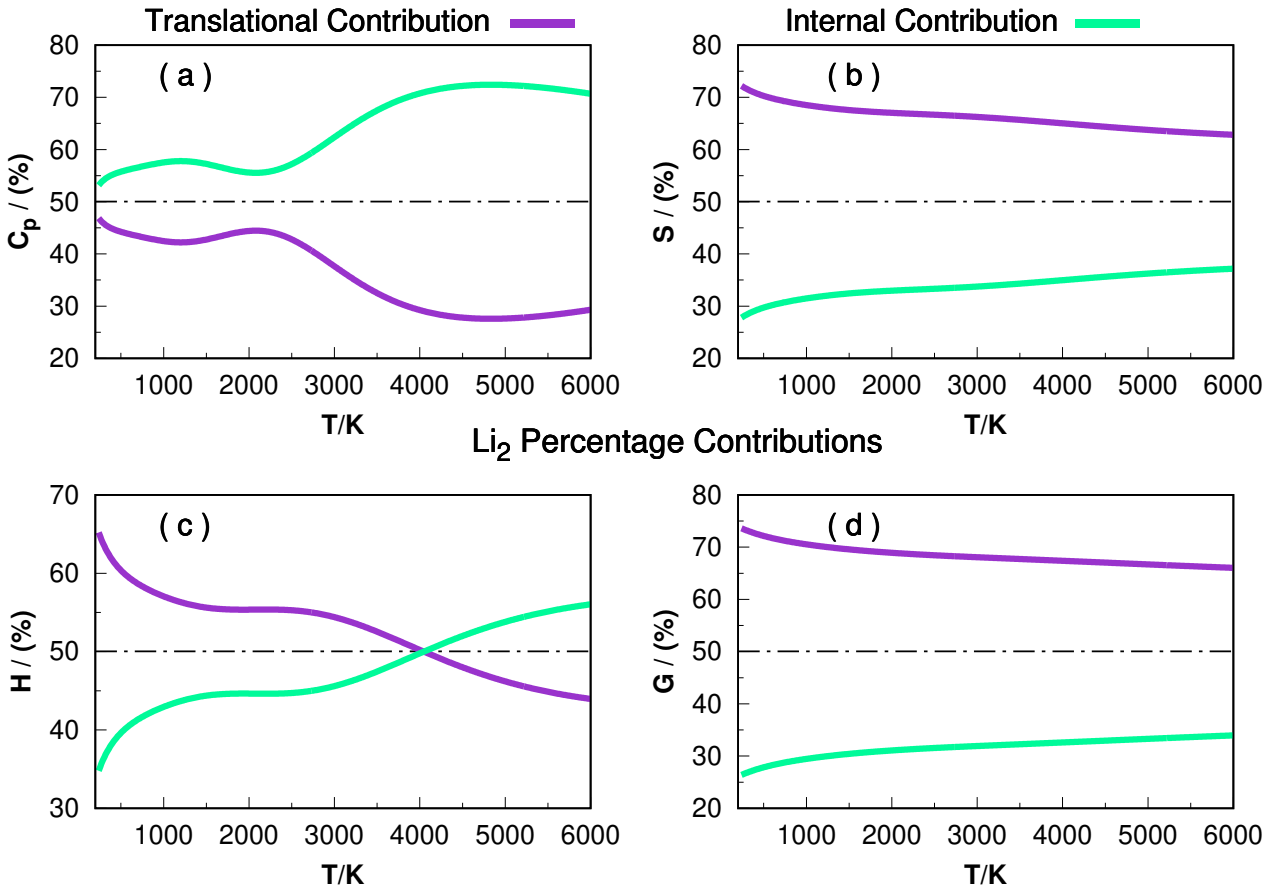

Figure S1: Percentage contribution of translational and internal degrees of freedom to the thermal properties of Li_2 at 1 atm pressure and different temperatures.

For the sodium dimer, a distinct thermal behavior is observed in C_p when analyzed across the temperature range from 300 to 5100 K. Notably, the internal contribution $C_{p,\mathrm{int}}$ exceeds the translational term $C_{p,\mathrm{tr}}$ from 300 up to 2050 K, indicanting an early and significant activation of internal states due to the ground state. Between 2050 K and 2540 K, however, a reverse

comportament is observed: the translational contribution becomes slightly greater than the internal one $C_{p,\mathrm{int}} < C_{p,\mathrm{tr}}$. This inversion suggests a relative stagnation in the activation rate of new internal degrees of freedom within this interval, while the translational contribution though constant in its ideal limit briefly dominates in relative terms. Above 2540 K, the internal heat capacity contribution once again surpasses the translational component $C_{p,\mathrm{int}} > C_{p,\mathrm{tr}}$, and continues to increase with temperature. This internal dominance becomes most pronounced at 5100 K, where the internal term accounts for a maximum of approximately 75.30% of the total heat capacity. Such behavior emphasizes the strong sensitivity of $C_p(\mathrm{Na_2})$ to thermal excitation of internal states at elevated temperatures. Regarding the enthalpy H, the translational component H_{tr} remains the dominant contributor up to 4530 K. Beyond this threshold, the internal enthalpy term H_{int} becomes predominant (see figure S2 in SM for more details).

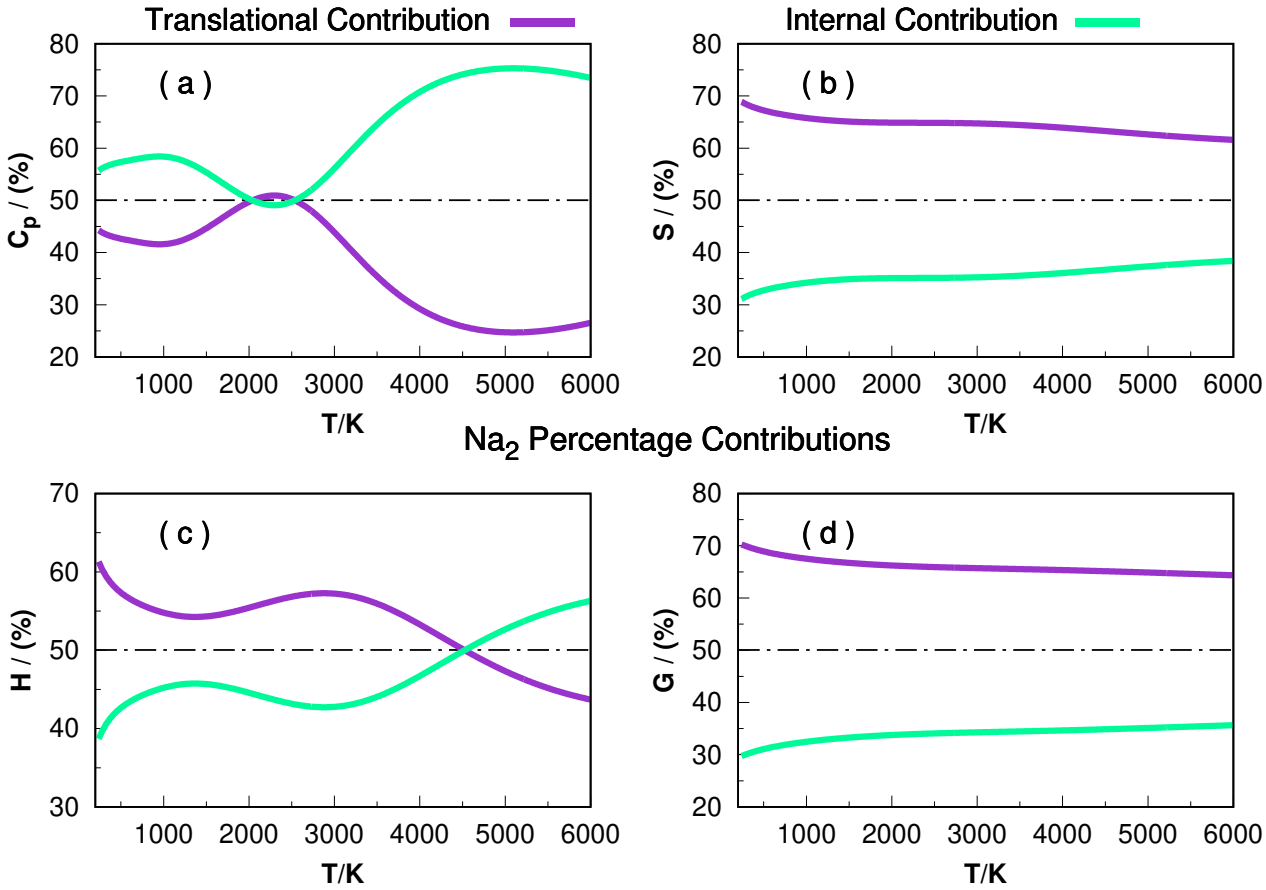

Figure S2: Percentage contribution of translational and internal degrees of freedom to the thermal properties of $\mathrm{Na_2}$ at 1 atm pressure and different temperatures.

For the thermal properties contributions of the potassium dimer $\mathrm{K_2}$ in 300 K to 1230 K, the $C_{p,\mathrm{int}}$ exceeds the translational component $C_{p,\mathrm{tr}}$. Between 1230 K and 2100 K, an inversion of this behavior is observed, with $C_{p,\mathrm{tr}}$ slightly surpassing $C_{p,\mathrm{int}}$ and the translational contribution H_{tr} remains the dominant term up to around 3650 K. Beyond this point, the internal contribution H_{int} becomes increasingly significant.

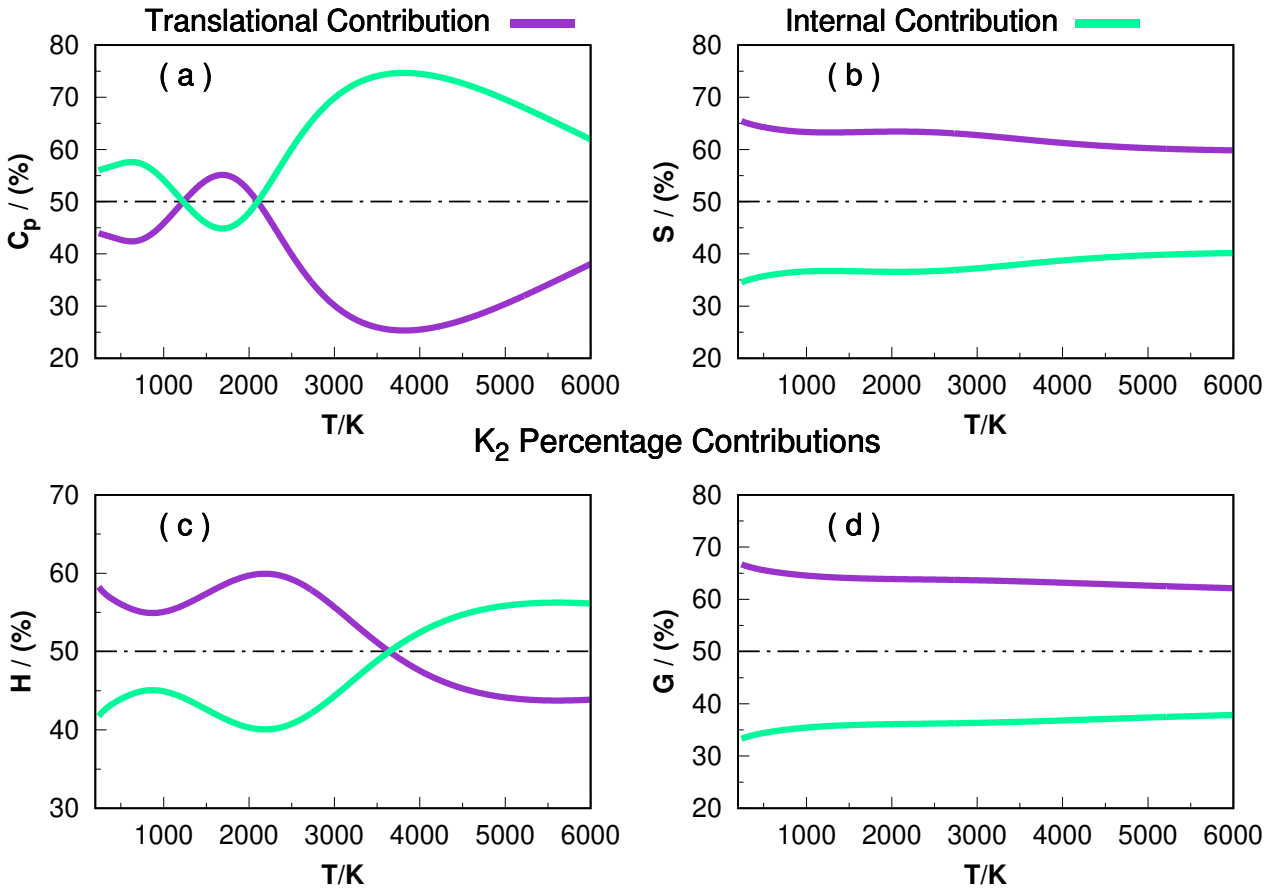

Figure S3: Percentage contribution of translational and internal degrees of freedom to the thermal properties of K_2 at 1 atm pressure and different temperatures.

The thermal behavior of the Rb_2 in 300K to approximately 1150K, the internal contribution $C_{p,\mathrm{int}}$ dominates over the translational part $C_{p,\mathrm{tr}}$. As the temperature increases beyond 1150K up to about 2080K, a crossover is observed where $C_{p,\mathrm{tr}}$ becomes slightly greater than $C_{p,\mathrm{int}}$. For the enthalpy H, the translational contribution H_{tr} remains the leading term up to approximately 3450K, above which the internal contribution H_{int} begins to prevail.

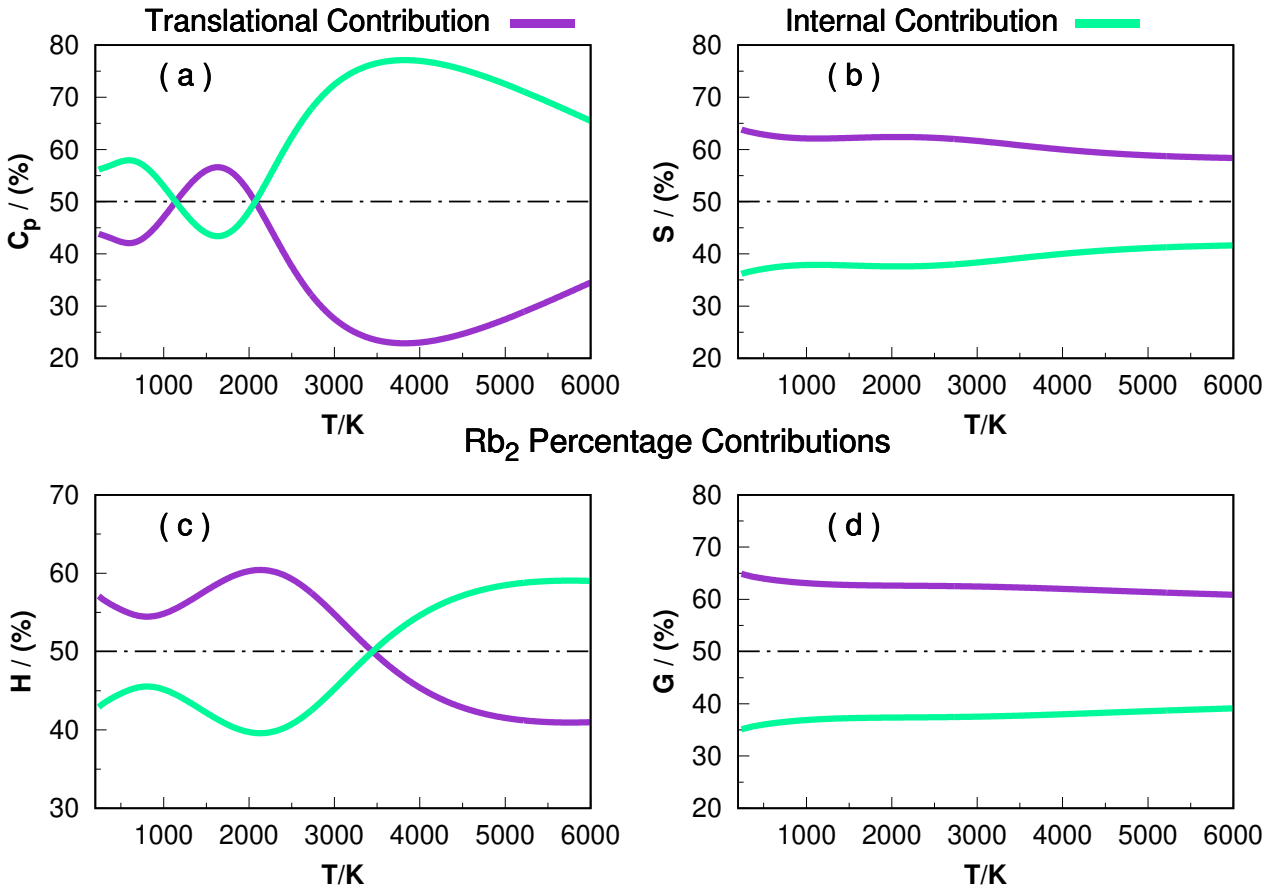

Figure S4: Percentage contribution of translational and internal degrees of freedom to the thermal properties of Rb_2 at 1 atm pressure and different temperatures.

For Cs_2 the results in the temperature regime 300K to approximately 1030K, the internal contribution $C_{p,\mathrm{int}}$ dominates over the translational part $C_{p,\mathrm{tr}}$. As the temperature increases beyond 1030K up to about 1570K, a crossover is observed where $C_{p,\mathrm{tr}}$ becomes slightly greater than $C_{p,\mathrm{int}}$, 5190K at 6000K the $C_{p,\mathrm{tr}}$ returns to become the greater term. For the enthalpy H, the translational contribution H_{tr} remains the leading term up to approximately 2450K, above which the internal contribution H_{int} begins to prevail.

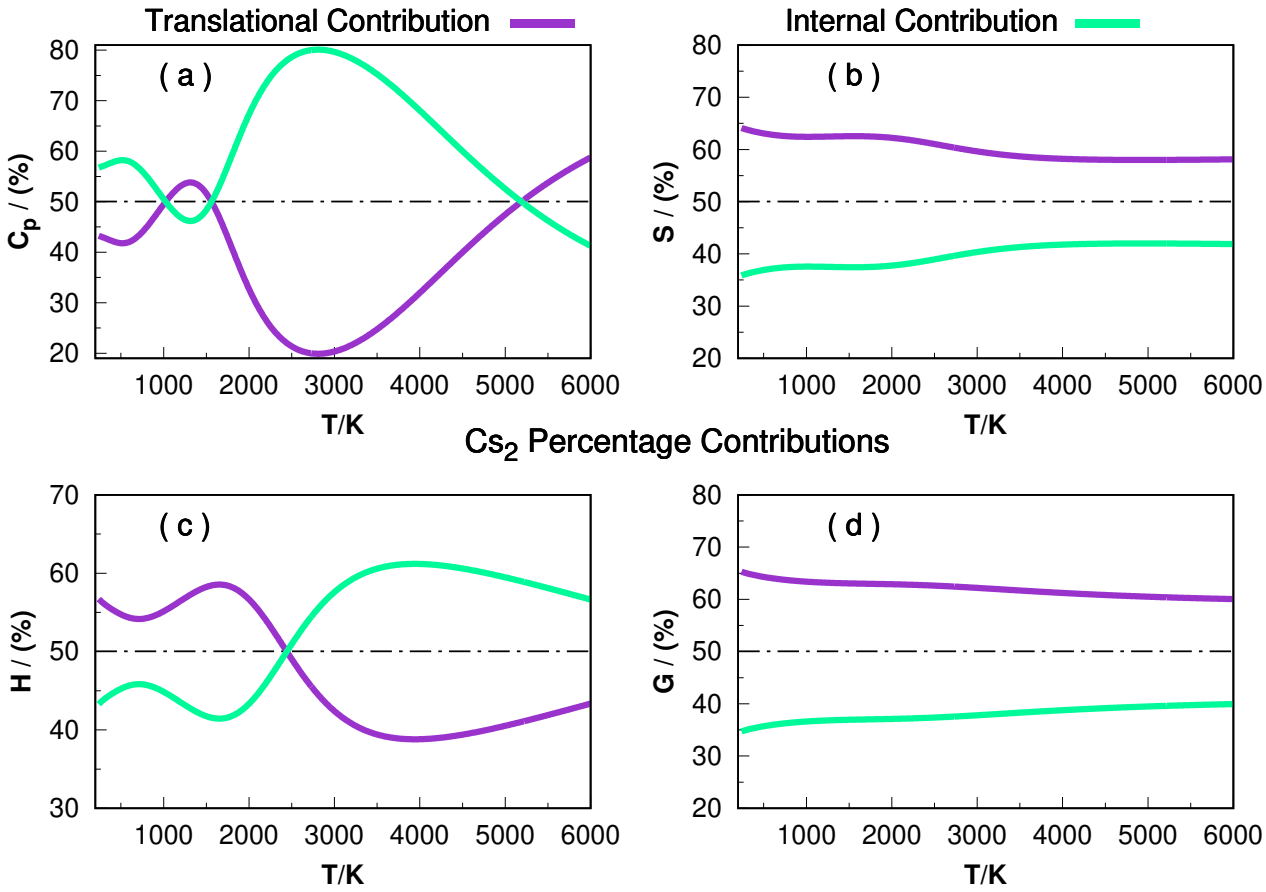

Figure S5: Percentage contribution of translational and internal degrees of freedom to the thermal properties of Cs_2 at 1 atm pressure and different temperatures.

And for Fr_2 in the temperature regime 300K to approximately 990K, the internal contribution $C_{p,\mathrm{int}}$ dominates over the translational part $C_{p,\mathrm{tr}}$. As the temperature increases beyond 990K up to about 1370K, a crossover is observed where $C_{p,\mathrm{tr}}$ becomes slightly greater than $C_{p,\mathrm{int}}$, 5520K at 6000K the $C_{p,\mathrm{tr}}$ returns to become the greater term. For the enthalpy H, the translational contribution H_{tr} remains the leading term up to approximately 2340K, above which the internal contribution H_{int} becomes predominant.

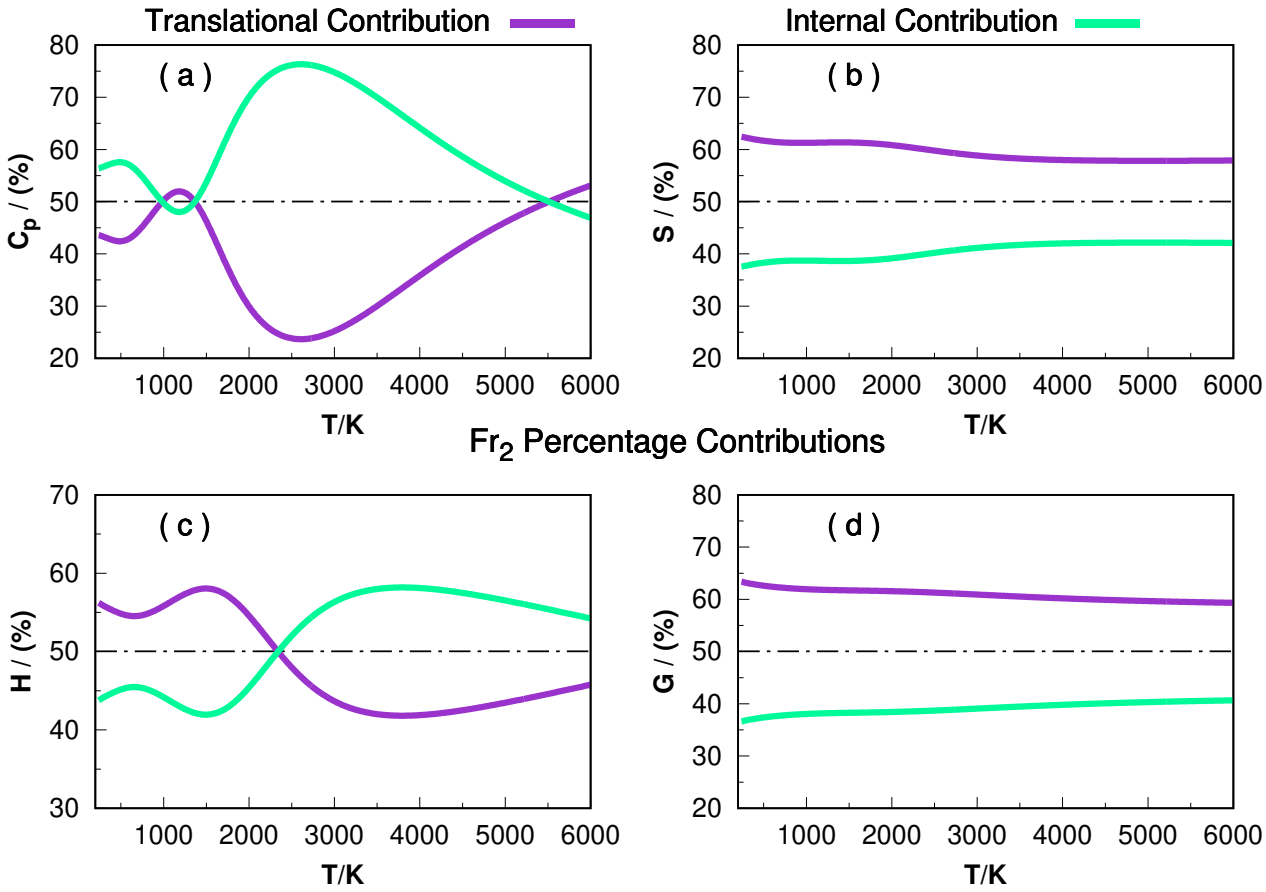

Figure S6: Percentage contribution of translational and internal degrees of freedom to the thermal properties of Fr_2 at 1 atm pressure and different temperatures.

2.9 Entropy Contribution of Low Lying States

To calculate the percentage contribution of the low-lying electronic states to the thermal property of entropy, we employed the Gibbs entropy equation based on the occupation probabilities derived from the partition function under thermal equilibrium for the alkali metal dimers. These probabilities, $\mathscr{P}_i$, correspond to the relative contributions of each electronic state to the total partition function. The entropy S is thus given by:

$$S(T) = -R \sum_i \mathscr{P}_i(T) \ln \mathscr{P}_i(T), \quad \text{where} \quad \mathscr{P}_i(T) = \frac{Q_i(T)}{\sum_j Q_j(T)} \tag{36}$$

where Q_i represents the partition function contribution of the i-th electronic state. The detailed results for these entropy contributions are presented below.

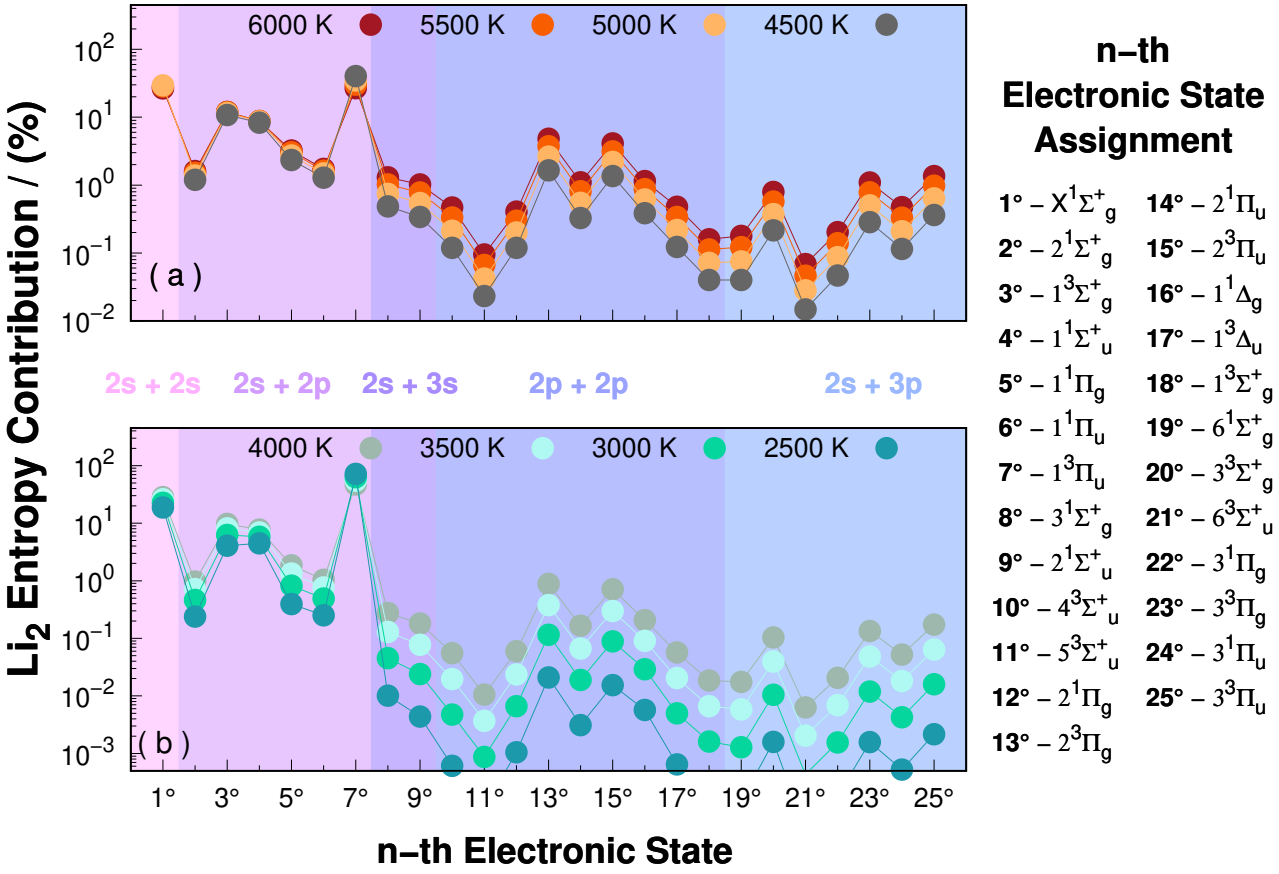

Figure S7: Entropy percentage of the n-th electronic state to the total internal partition function of Li_2 at different temperatures.

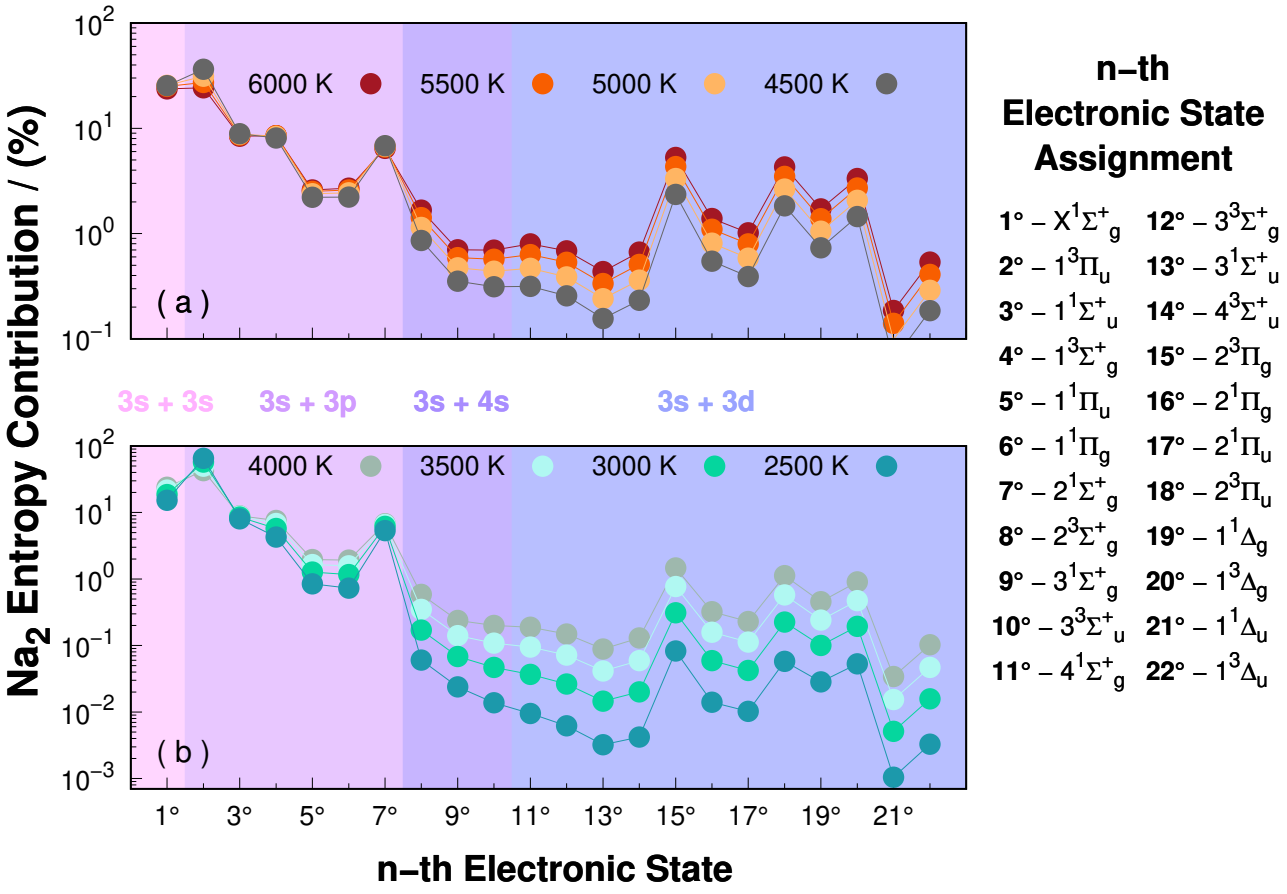

Figure S8: Entropy percentage of the n-th electronic state of Na_2 at different temperatures.

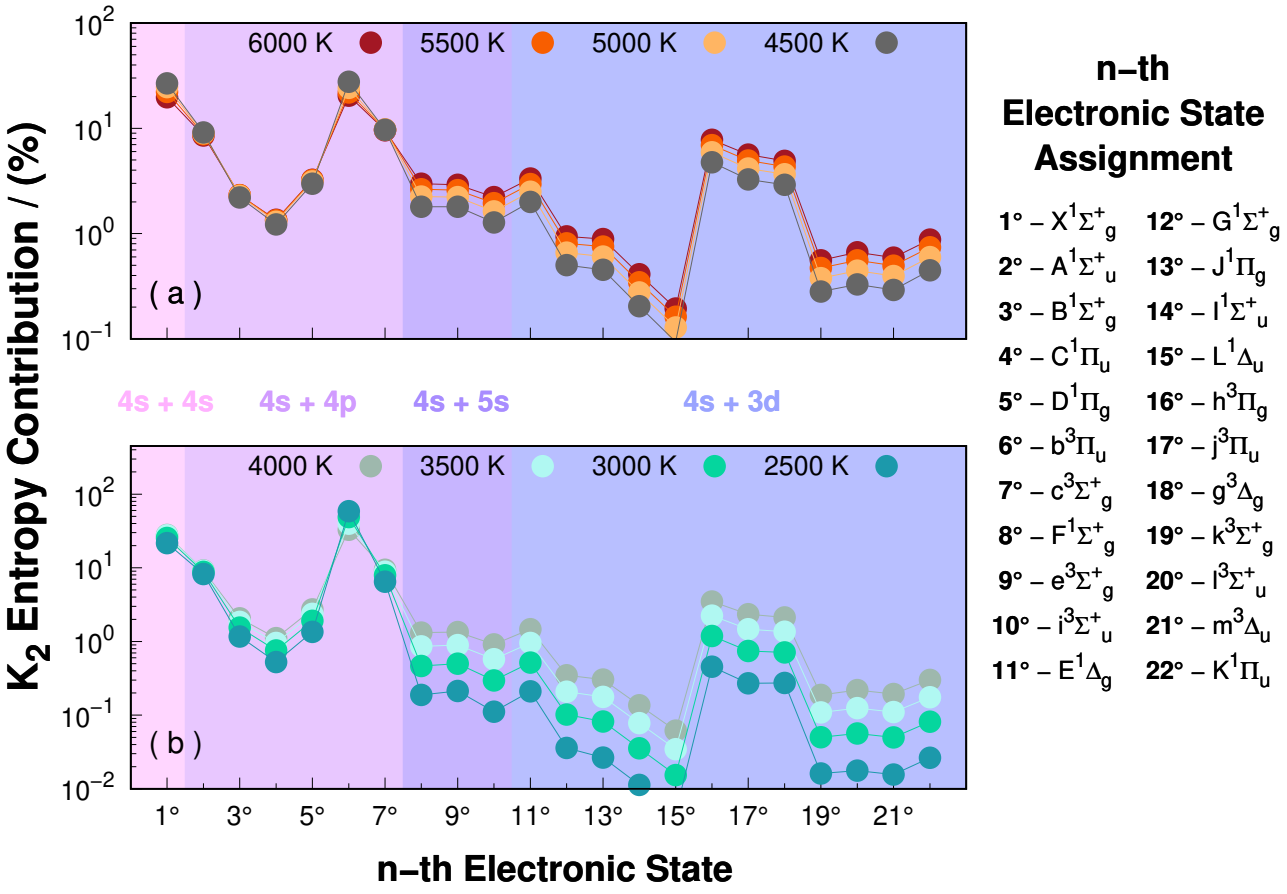

Figure S9: Entropy percentage of the n-th electronic state to the total internal partition function of K_2 at different temperatures.

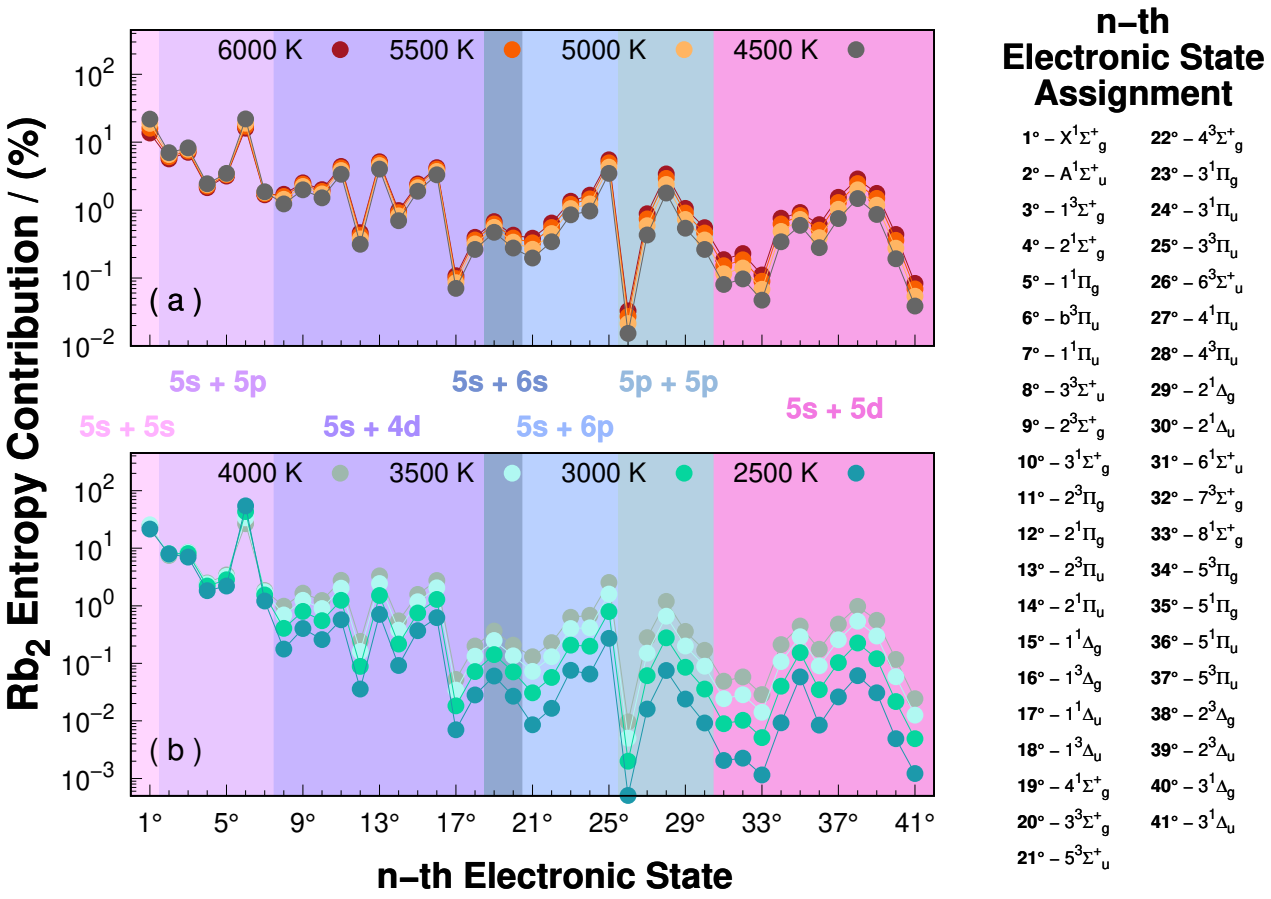

Figure S10: Entropy percentage of the n-th electronic state to the total internal partition function of Rb_2 at different temperatures.

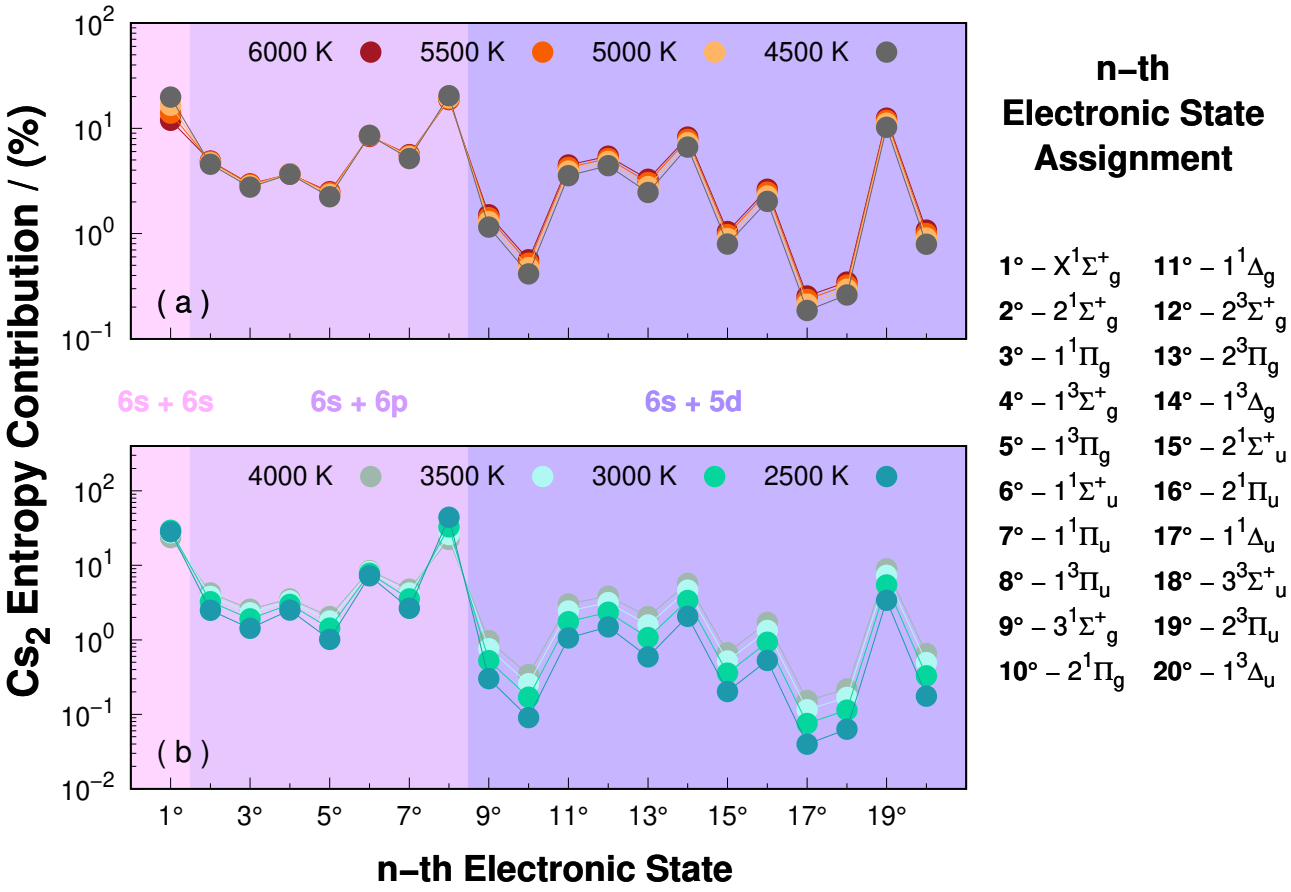

Figure S11: Entropy percentage of the n-th electronic state to the total internal partition function of Cs_2 at different temperatures.

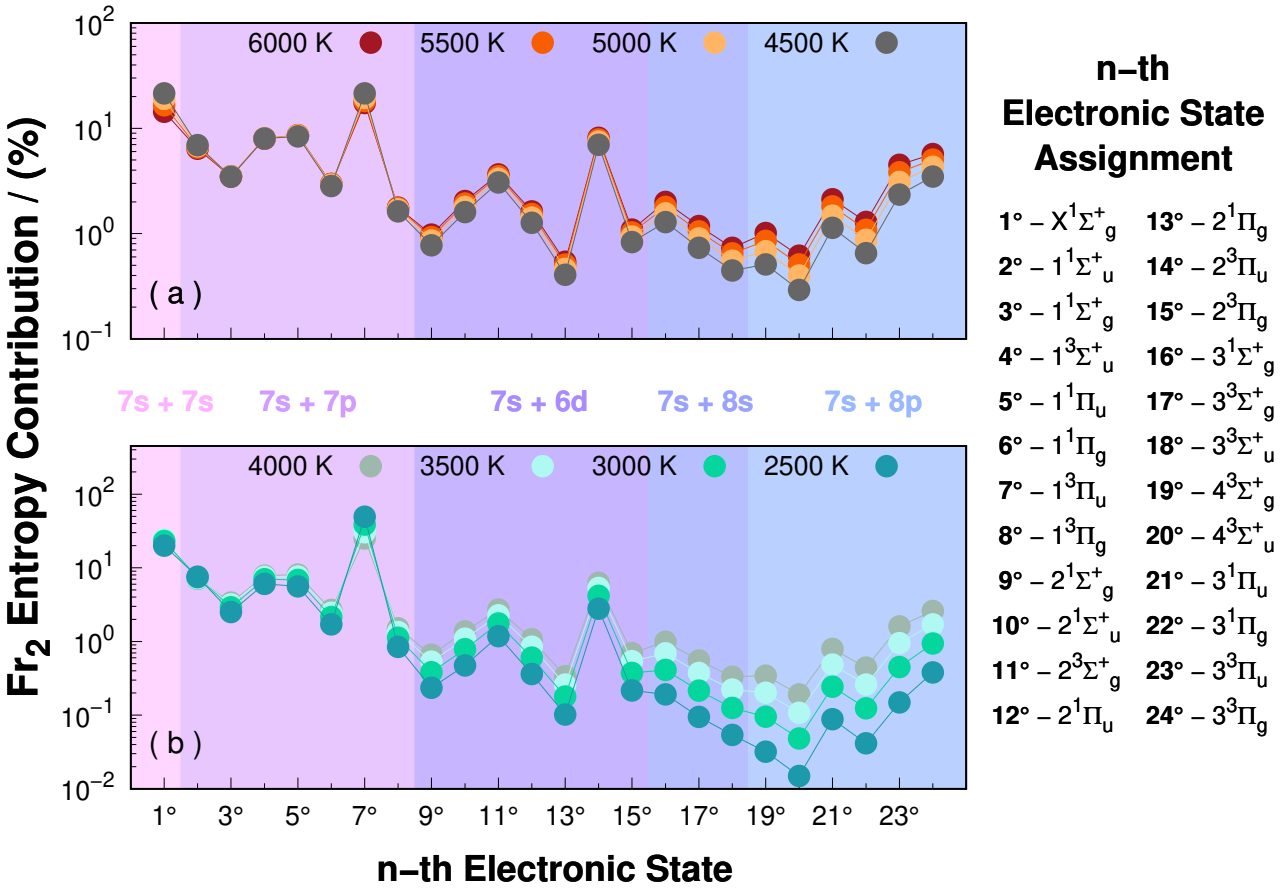

Figure S12: Entropy percentage of the n-th electronic state to the total internal partition function of Fr_2 at different temperatures.

From a statistical physics perspective, the behavior of the percentage contributions of electronic entropy exhibits a direct and strong dependence on the thermal population probabilities of the electronic states. At low temperatures, the system predominantly occupies the electronic ground state, whose probability asymptotically approaches unity as the temperature tends to zero. Consequently, the configurational disorder associated with the electronic degrees of freedom vanishes, leading to a null contribution to entropy from the ground state under these conditions. As the temperature increases, the thermal energy becomes sufficient to overcome the energy gaps between the electronic states, rendering excited states progressively accessible. This enhanced accessibility results in a redistribution of the occupation probabilities among the available states, thereby increasing the electronic entropy. The behavior of the entropy is therefore intrinsically analogous to the statistical distribution of the electronic state populations governed by the Boltzmann factor. In summary, the electronic entropy displays a highly temperature dependent profile: it remains negligible at low temperatures due to the dominance of the ground state, and progressively increases as higher electronic states become thermally populated. This trend consistently mirrors the probability distribution of the electronic states as a function of temperature.

2.10 Partition Function of Alkali Metals

The total partition function for the alkali metal dimers was computed using the quantum statistical method 1 adopted in this work, considering only the bound electronic states. Fig-

ure S13 presents the results for the partition function as a function of temperature. The solid lines represent calculations that include all bound electronic states considered in this study, while the dotted points correspond to the partition function evaluated using only the electronic ground state. It is evident that the inclusion of excited electronic states leads to a significant increase in the partition function, especially at higher temperatures. Additionally, a clear periodic trend is observed along the alkali metal series, with heavier dimers exhibiting larger partition function values. This behavior reflects the increasing density of accessible internal states for heavier species, contributing to enhanced thermodynamic activity. These results highlight the critical role of electronic excitation in accurately describing the thermodynamics of alkali metal dimers.

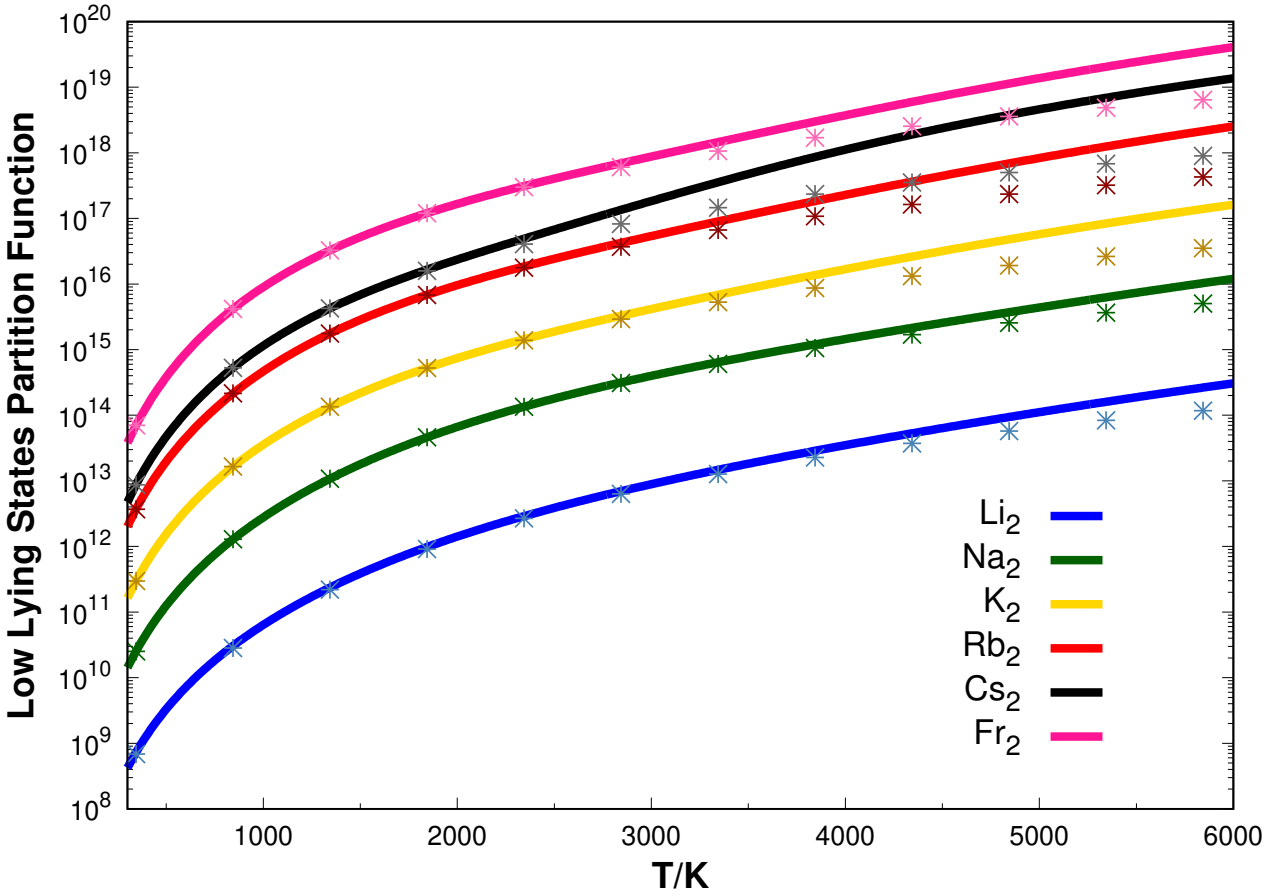

Figure S13: Total Low Lying Partition Function of Alkali Metals with ideal gas model.

2.11 Excluding Negative Terms from the Molecular Partition Function: A Numerical Justification

In the classical formalism, the internal partition function for a diatomic molecule interacting via an effective potential $U_n(r)$ is given by:

$$Q_{\text{int}}^{cl}(\beta) = \frac{g_n}{2\sqrt{\pi}} \left(\frac{2\mu}{\beta}\right)^{3/2} \int_0^\infty [\exp(-\beta U_n(r)) - 1]\, r^2\, \mathrm{d}r. \tag{37}$$

This integral includes contributions from both attractive and repulsive regions of the potential. However, unlike in the quantum formulation, the classical expression does not inherently

distinguish bound from unbound states. The classical integral can be separated into two parts: $Q_{\text{int}}^{cl}(\beta) = Q_N(\beta) + Q_{NE}(\beta)$, according to Ref.[8] where:

$$Q_N(\beta) = \frac{g_n}{2\sqrt{\pi}} \left(\frac{2\mu}{\beta}\right)^{3/2} \int_0^{\sigma} \left[\exp(-\beta U_n(r)) - 1\right] r^2 \, \mathrm{d}r, \tag{38}$$

$$Q_{NE}(\beta) = \frac{g_n}{2\sqrt{\pi}} \left(\frac{2\mu}{\beta}\right)^{3/2} \int_{\sigma}^{\infty} \left[\exp(-\beta U_n(r)) - 1\right] r^2 \, \mathrm{d}r. \tag{39}$$

The term $Q_N(\beta)$ is strictly negative due to the exponential suppression in the repulsive region ($\exp(-\beta U_n(r)) \ll 1$ when $U_n(r) \gg 0$). To quantitatively assess the influence of this term, we define the ratio $R(\beta) = |Q_N|/Q_{NE}$ which measures the magnitude of the negative repulsive contribution relative to the physically meaningful non-repulsive region. When $R(\beta) \ll 1$, the repulsive term is negligible, and its exclusion does not affect the physical predictions of the model. To further illustrate the negligible role of the repulsive region, we consider the hard sphere model for analyses of ground electronic states in the purelly repulsive region:

$$U_n(r) = \begin{cases} \infty, & 0 \leq r < \sigma \\ 0, & r \geq \sigma \end{cases} \tag{40}$$

Substituting this into the classical partition function:

$$\begin{aligned} Q_{NHS}(\beta) &= \frac{g_n}{2\sqrt{\pi}} \left(\frac{2\mu}{\beta}\right)^{3/2} \int_0^{\sigma} \left[\exp(-\beta U_n(r)) - 1\right] r^2 \, \mathrm{d}r \\ &= \frac{g_n}{2\sqrt{\pi}} \left(\frac{2\mu}{\beta}\right)^{3/2} \int_0^{\sigma} \left[0 - 1\right] r^2 \, \mathrm{d}r \\ &= -\frac{g_n}{2\sqrt{\pi}} \left(\frac{2\mu}{\beta}\right)^{3/2} \int_0^{\sigma} r^2 \, \mathrm{d}r \\ &= -\frac{g_n}{6\sqrt{\pi}} \left(\frac{2\mu}{\beta}\right)^{3/2} \sigma^3. \end{aligned} \tag{41}$$

This expression shows that the repulsive contribution has a simple analytical form, which is purely negative and scales with σ^3. Its magnitude decreases rapidly with increasing temperature and mass, as expected for a term dominated by a volume exclusion effect.

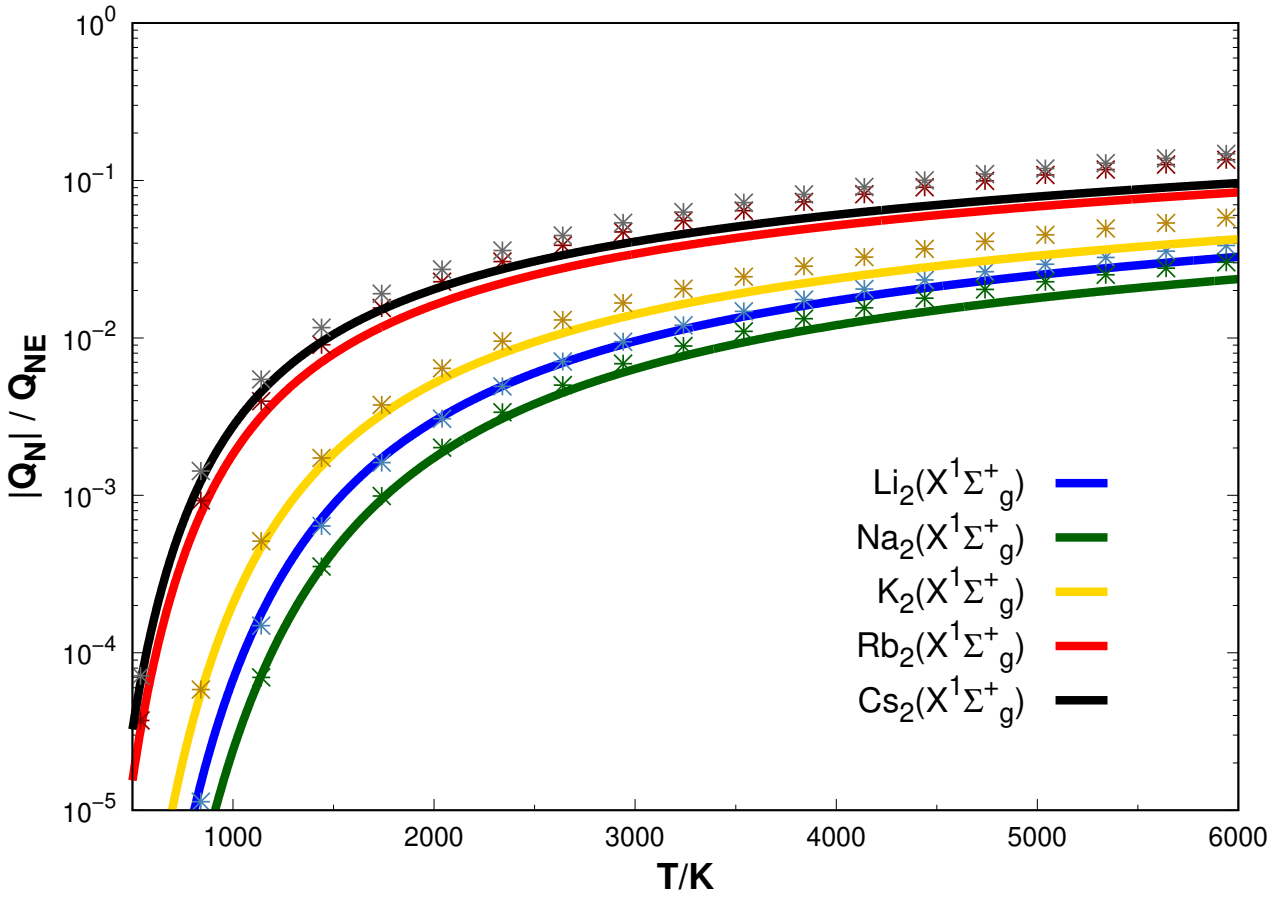

Figure S14: Classical partition function Ratio $|Q_N|/Q_{NE}$ as a function of temperature. The dashed line indicates the results with hard sphere model for the Q_N function.

At low temperatures, Q_{NE} dominates due to the prevalence of bound configurations, while Q_N remains small and at high temperatures, although both terms increase, their relative ratio stabilizes and remains below unity in most physically relevant cases. These results provide both a numerical and conceptual justification for excluding the negative repulsive contribution from the internal partition function, the results also show that the hard sphere model can describe the negative contribution of the classical partition function at moderate temperature range [8, 9]. Doing so yields a more physically meaningful result that accurately reflects only the accessible, bound configurations of the molecular system. Moreover, this classical analysis offers insight into the quantum case. Since the classical and quantum partition functions converge in the high-temperature limit, and the repulsive classical term is negligible at low temperatures where bound states dominate, it is therefore consistent to construct the quantum partition function using only the bound energy levels. This approach avoids the inclusion of unbound continuum states and aligns with the thermodynamic behavior observed classically.

Furthermore, for low-lying electronic states with sufficiently deep potential wells, it is reasonable to assume analogies with the behavior of the electronic ground state at moderate temperatures, particularly regarding the negative contribution to the partition function. In such cases, the negative term Q_N is expected to be significantly smaller than Q_{NE}, which supports the predominance of Q_{NE} in this regime. On the other hand, for electronic states associated with shallow potential wells, it may occur that Q_N exceeds Q_{NE} at high temperatures. Nevertheless, when considering a thermal regime in which multiple electronic states are accessible, the total sum of all Q_{NE} contributions from the available states tends to be significantly greater

than the sum of all corresponding Q_N terms of n electronic state. Therefore, it is a reasonable assumption to consider that $\sum_n Q_{NE}^n \gg \sum_n Q_N^n$ over a wide temperature range.

References

[1] António JC Varandas and José Dias da Silva. Potential model for diatomic molecules including the united-atom limit and its use in a multiproperty fit for argon. *J. Chem. Soc., Faraday Trans.*, 88(7):941–954, 1992.

[2] Marcin Buchowiecki. High-temperature heat capacity of the Na_2 molecule. *International Journal of Thermophysics*, 40(7):70, 2019.

[3] Marcin Buchowiecki. Vibrational partition function for the multitemperature theories of high-temperature flows of gases and plasmas. *J. Phys. Chem. A*, 124(20):4048–4052, May 2020.

[4] Frederick H. Mies and Paul S. Julienne. The thermodynamic properties of diatomic molecules at elevated temperatures: Role of continuum and metastable states. *The Journal of Chemical Physics*, 77(12):6162–6176, December 1982.

[5] M. Capitelli and U. Lamanna. Second virial coefficients of oxygen—oxygen and carbon—oxygen interactions in different electronic states. *Chemical Physics*, 14(2):261–266, 1976.

[6] Alan W. Irwin. Refined diatomic partition functions. i – calculational methods and h_2 and co results. *Astron. Astrophys.*, 182(2):348–358, August 1987.

[7] Jr. Chase, Malcolm W. *NIST-JANAF Thermochemical Tables.* Journal of Physical and Chemical Reference Data, Monograph No. 9. American Chemical Society; American Institute of Physics for the National Institute of Standards and Technology, Washington, DC; New York, 1998.

[8] Marcin Buchowiecki and. On the exclusion of the negative contribution to the molecular partition function. *Molecular Physics*, 117(13):1640–1644, 2019.

[9] Marcin Buchowiecki. Influence of scattering on the vibrational partition function at extreme temperatures. *The European Physical Journal Plus*, 136(2):245, 2021.